Desalination and Water Treatment
www.deswater.com

doi:10.5004/dwt.2019.24148

159 (2019) 338–345
August

Detection and removing of lead from wastewater using chemical treatment of polyurethane foam waste: Batch and column experiments

E.A. Moawed*, M.A. El-Hagrasy, M. Kamal

Chemistry Department, Faculty of Science, Damietta University, P.O. Box: 34517, Damietta, Egypt, Fax 0020572403868, email: eamoawed@yahoo.com (E.A. Moawed), m_el_hagrasy@yahoo.com (M.A. El-Hagrasy), mohamedkmal1989@gmail.com (M. Kamal)

Received 23 October 2018; Accepted 20 March 2019

ABSTRACT

A new inexpensive sorbent was prepared from the waste of polyurethane foam (PUF) which highly surface polarity and sorption capacity. PUF was modified by adding amino, chloro and hydroxyl groups to its matrix. The polyamine polyhydroxy polyurethane chloride (PPPC) was characterized by using elemental analysis (EA), bulk conductivity (BC,σ), infrared/ultraviolet/visible spectra (IR/UV/Vis), pH point zero charge (pH_{ZCP}), thermal analysis (TGA/DTA/DSC), scanning electron microscope (SEM) and X-ray diffraction (XRD). The PPPC owned improved stability in acidic/alkaline solutions and organic solvents. The pH_{ZPC} of PPPC was 5.1 and the maximum values of ΔpH of PPPC are + 1.5 and –3.8 at pH 3.2 and pH 8.3. The σ of PPPC was 2.6×10^{-5} $\Omega^{-1}m^{-1}$. PPPC contains several active groups (NH_2, Cl, OH, C=O, C=C, and C-O-C) which classified as an effective sorbent for the solid-phase extraction (SPE) of Pb(II) ions from wastewater. The removing rate of the Pb(II) ions onto PPPC was very fast with half-life time ($t_{1/2}$) 1.13 min at pH range 3–7. The value of ΔH for the sorption Pb(II) ions were –22.9 kJ/mol; these revealed that the values the extraction process is exothermic in nature. The recovery percentage of Pb(II) ions are 99–105% with relative standard deviation (RSD) 2.49% (n = 7).

Keywords: Polyurethane foam; Removal; Lead; Nile water; Wastewater

1. Introduction

Water pollution has become a severe worldwide problem which represents a serious risk for human health. Water resources contamination like heavy metals increases with time due to overpopulation, industrial renaissance and geological processes. Most compounds of heavy metals e.g. mercury, cadmium, lead, chromium, arsenic, zinc, copper, nickel, cobalt is non-biodegradable and causing organs damage [1–3]. Lead is very important elements in body metabolism at limited concentration, but, at over limit concentration it can be toxic and can cause bad effects to many biological and biochemical processes [4–6]. The heavy metals which directed to water resources may produce from industrial wastewater such as batteries, refining ores, alloy, electronics and electroplating. Because of heavy metals hazardous effects, even small concentrations of heavy metals can make human and environmental health risk. So, the removal of heavy metals from aqueous solutions is a very importance issue [7–9]. There are many methods for removing heavy metals as ion exchange, nanofiltration, precipitation, reverse osmosis and adsorption but among these methods solid phase extraction is still favorite one due to low cost, simplicity and potential for overcoming the environmental problems [10–12]. Polyurethane foam is one of the most important polymers materials, which has unique properties make it use in various fields [13,14]. Polyurethane foam materials are used widely, inevitably leading to a large number of polyurethane foam wastes production [15]. Worldwide, more and more attention is being focused on polyurethane recycling due to on-going changes in both regulatory and environmental issues.

*Corresponding author.

Increasing landfill costs and decreasing land-fill space is forcing consideration of alternative options for the disposal of polyurethane materials. Polyurethane is successfully recycled from a variety of consumer products, including: appliances, automobiles, bedding, carpet cushion, upholstered furniture [16]. PUF is a suitable sorbent that has been used for the solid phase extraction of both metal ions and organic compounds from different environmental samples. The importance of PUF as a sorbent is due to its low cost, sorption capacity, handling, and storage [17,18]. Also, polyurethane has advantages more than any other sorbent as PUF can directly use without previous treatment, a lot of chelating agents and liquid ion exchangers have been immobilized on it beside the number of possible sorption mechanisms can happen [19]. Polyurethane is a good material because of its high stability not only in acidic and basic media but also in organic solvents [20]. It was widely employed in different forms, as composite, incorporated, immobilized or coupled with many ligands. The high density of PUF/ligand is problematic since it decreases the sorption capacity of PUF and consequently lowers its extraction rate of metal ions. This problem demands the preparation of low density PUF with high polarity and high sorption capacity; this would be achieved by the replacement of the surface isocyanate groups by new chelating groups**.** Polyhydroxy polyurethane foam (PPF) is one of the PUF derivatives and can be prepared easily from the low-density PUF [21,22]. The PPF has low-density, high sorption capacity, low cost and has the ability to be recycled many times without a significant decrease in its sorption capacity. PPF was successfully employed for the selective removal of many metal ions from aqueous solutions [23]. Thus, this research article is focused on: (i) developing new polyurethane by the addition of amino and chloro groups to PPF matrix. Based on the improvement of the surface properties, offered by the increase of its polarity, we examined the ability of PPPC sorbents to be recycled many times without any significant decrease in their capacities. (ii) Studying of sorption kinetics, thermodynamics and other sorption parameters of iron, lead and zinc metal ions from the aqueous medium. (iii) Applicability of modified sorbent to remove iron, lead and zinc ions from wastewater.

2. Experimental

2.1. Apparatus

Measurements of the studied heavy metal ions were carried out using flame atomic absorption spectrophotometer (FASS) AA240FS (Varian, Australia). UV-Vis spectra of PPPC were performed on a JASCO (V-630 UV-VIS spectrophotometer, Japan). The pH measurements were carried out using a symphony pH-meter (USA) provided with a glass electrode. SEM was carried out using JEOL model JSM-6510LV apparatus, manufactured in USA. IR spectra were carried out using KBr disc on a JASCO FTIR-410 spectrometer in the 4000–400 cm^{-1} regions. The XRD patterns of the PPPC was recorded by X-ray diffractometer (Brucker D8 model) using anode Material Cu Kα radiation (λ = 1.5406 Å) at a generator voltage of 40 kV and a generator current of 40 mA. Thermal gravimetric analysis and differential scanning calorimetry [TGA-DSC] analysis were carried out using a simultaneous DSC-TGA device model (SDTQ 600, USA) under N_2 atmosphere with a heating rate of 10°C min^{-1}.

2.2. Reagents and materials

Chemical treatment of polyurethane foam (CT-PUF): The flexible polyurethane foam wastes in different densities (PUF) were cut to small pieces and soaked in 2 mol/L of HCl for 24 h to remove dust and other impurities. The PUF pieces were boiled in HCl (3 mol/L) at 2 h to reduce the nitrous groups and also to liberate the free amino groups. The CT-PUF were washed with distilled water and dried in air followed by ground in a food-processing blender.

Polyamine polyhydroxy polyurethane chloride (PPPC): 10 g of CT-PUF were kept in HCl (0.1 mol/L) in an ice bath then diazotized with 50 mL of $NaNO_2$ (2 mol/L) to form PUF-$N_2^+Cl^-$ salt. To replace the azo groups by hydroxyl groups; the product was boiled with distilled water. The PPF was boiled with 2 mol/L HCl then diazotized by adding 50 mL of $NaNO_2$ (2 mol/L) followed by added 50 mL of CuCl solution (0.3 mol/L). PPPC material was washed with distilled water followed by acetone and finally air-dried.

Stock solution (1000 ± 2 mg/L) of the Pb(II) was prepared by dissolving appropriate amounts of $Pb(NO_3)_2$ (Merck, Germany) in bidistilled water containing 1 mL concentrated HNO_3. A series of 25 mL for metal standard solutions (0–3 mg/L) was used for the preparation of the calibration curve.

2.3. Recommended procedures

Parameters such as pH, contact time, initial metal ions concentration and temperature for adsorption of Pb(II) was carried out by using batch experimental. A series of 100 mL conical flasks containing 25 mL of Pb(II) solution of known pH, concentration was shaken with 0.1 g of PPPC (pH of the solutions was adjusted using 0.1 mol/L CH_3COOH/NaOH). Blank solutions were run under the same conditions except for the addition of PPPC. After 1 h, the solution samples were filtered and the concentration of the remaining and the recovered from the PPPC was estimated using FASS. The percentage of removing metal ions (%E) and the capacity of PPPC (Q) were calculated by the following equations:

$$\%E = \left(\frac{C_o - C}{C_o}\right) \times 100 \quad (1)$$

$$Q = \frac{C_o E V}{m} \quad (2)$$

In dynamic experiments, 1.0 g portion of PPPC was packed into a column (15-cm long, 1.5 cm in diameter and L = 8 cm) then 25 mL of Pb(II) solution (1 mg/L) was passed through the PPPC column at a flow rate of 2 mL/min then the Pb(II) ions was eluted using 0.05 mol/L CH_3COOH. Effluents and eluted Pb(II) ions from the PPPC column were determined by FASS.

3. Results and discussion

3.1. Characterization of PPPC

FTIR spectra of PUF, PPF and PPPC were recorded in the region between 400 and 4000 cm^{-1} (Fig. 1). The stretching vibrations band absorb at 3220 cm^{-1} in the PUF spectrum was shifted to 3255.3 cm^{-1} then to 3322.7 cm^{-1} in PPF and PPPC, respectively. This shifted of the band in the spectra of PPF and PPPC is due to adding of OH group. The new stretching vibrations bands at 403, 449 and 514 cm^{-1} assigned to C–Cl group have appeared in the PPPC spectrum. The spectrum of PPPC revealed that the broadband was observed at 3083–3683 cm^{-1} and also several stretching and bending vibrations bands at 2930, 2858, 1714, 1600, 1565, 1517, 1367, 1214 1079 and 682 cm^{-1}. This result showed that the PPPC contains several active groups e.g. N-H, O-H, $C\text{-}H_{Ar}$, $C\text{-}H_{Al}$, C=O, C=C, C-O-C and C-Cl groups. The $\upsilon_{(OH)}$ of the PPPC at 3322.7 cm^{-1} was shifted to 3265 cm^{-1} after the sorption of Pb(II) ions. This may point to the role of the phenolic –OH group of the PPPC on the sorption process. In addition, the new bands were developed at 437 and 478 cm^{-1} (C-M group), indicating the reaction of PPPC with these metal ions forming PPPC: Pb(II).

The amino, chloro, and phenolic groups presence in PPPC were chemically detected using $NaNO_2$/β-naphthol; Na metal/$AgNO_3$ and $FeCl_3$/HCl solutions. The formation of an orange-red azo dye, white precipitate or violet color indicated the presence of amino, chloro, and phenolic groups. The phenolic sites in PPPC were estimated by back titrated with 0.05 mol/L of NaOH/HCl; the determined phenolic sites of PPC are 0.4 mmol OH/g.

The electronic spectra of PUF, PPF, and PPPC were recorded using Nujol mulls method (Fig. 2). The UV spectrum of PUF shows that the band has appeared between 200 and 204 nm assigned to the π-π* transitions localized on the conjugated system (Fig. 3). The spectrum of PPF contains broadband from 200 to 230 nm due to the inner bonding of OH groups and peak at 382 nm due to n-π*. While the PPPC spectrum contains many sharp peaks at 204, 206, 213, 219, 224, 226, 232 and 236 nm due the several functional groups of PPPC has π-π* transition. Also, PPPC contains many sharp peaks at 329, 331, 336, 343, 346, 351, 356, 365, 373, 375 and 379 nm are due to n-π* transition (Fig. 3). The higher energy peaks PPPC from 204 nm to 236 nm are assigned to the intra ligand transitions (π-π*) that are localized on the conjugated system and are consumed by complexation with Pb(II) ions.

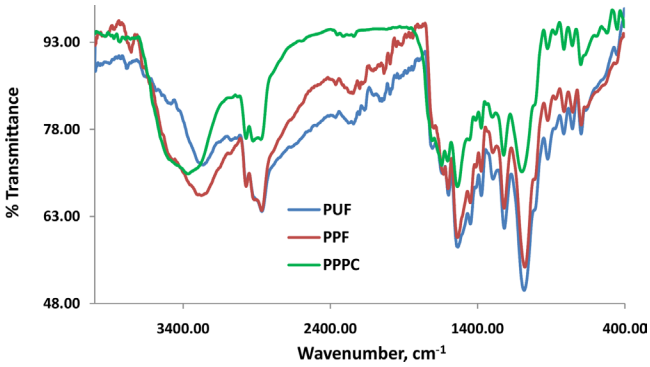

Fig. 1. Infrared spectrum of PUF, PPF & PPPC.

The lower energy peaks of PPPC from 329 nm to 379 nm are red-shifted to bands at 348–392 nm after the sorption of Pb(II) ions. The lower energy peaks of PPPC are assigned to n-π* transition of the OH, NH and C=O chromophores that overlapped with the charge-transfer (CT) transitions within the molecule. The results showed that the shifted of spectral bands of PPPC are due to the reaction with Pb(II) ions. From the results of the electronic and infrared spectra of the PPPC before and after Pb(II) sorption, we suggest that the sorption of lead(II) ions on PPPC occurs principally according to chelation mechanism via the coordination of amino, chloro, phenolic and carbonyl groups with Pb(II) ions.

The surfaces properties of PUF, PPF and PPPC were confirmed by XRD pattern; broad diffraction bands are observed at 19.25, 19.65 and 21.25° with the halo from 4 to 80° (Fig. 3). These broad bands confirmed that PUF, PPF, and PPPC surfaces are the amorphous structure which usually observed for the PUF matrix. XRD diffraction pattern of PPPC has some intense peaks (16.59°, 32.89°, 40.21°, 50.58°, and 54.08°) compared to PUF and PPF, which show some degree of crystallinity in PPPC structure (Trovati et al., 2010). The observed XDR pattern for the PPPC indicates that the substitution of amino, chloro, and hydroxyl groups into PPPC caused a phase change from completely amorphous phase to the phase crystalline polymer. The spacing between diffracting planes of PPPC was calculated by using Bragg's law: $2d \sin\theta = n\lambda$ where d is the spacing between diffracting planes, θ is the incident angle, n is an integer, and λ

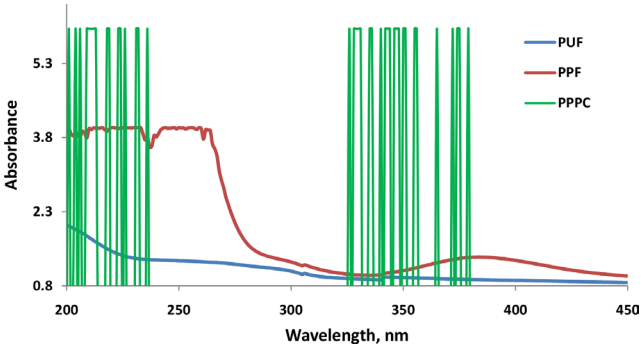

Fig. 2. UV spectrum of PUF, PPF and PPPC.

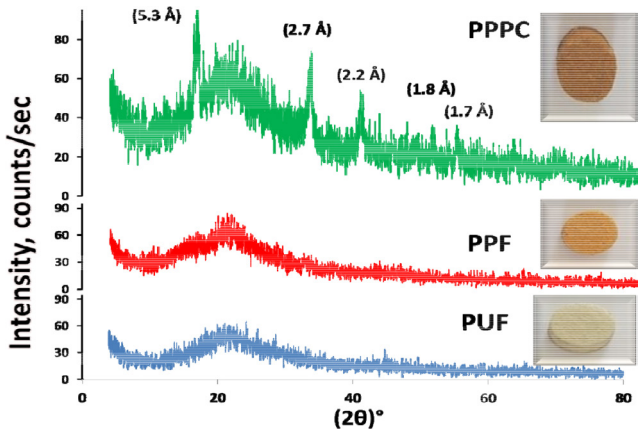

Fig. 3. XDR of PUF, PPF and PPPC.

is the wavelength of the beam. The *d* values of PPPC are 5.3, 2.7, 2.2, 1.8 and 1.7 Å.

The values of pH_{PZC} of sorbents are mainly depending on the matrix structure and the terminal groups. The pH_{PZC} values for PUF, PPF and PPPC are 1–7.5, 5–7.4 and 5.1, respectively (Fig. 4). These values show that the surface of PPPC is highly affected by the solution medium. At pH value < 5.1, the surface of the PPPC would be positively charged while at pH value > 5.1, the surface of the PPC would be negatively charged. The ΔpH values of PPPC are +1.5 and –3.8 at pH 3.2 and pH 8.3, respectively (Fig. 5). While the ΔpH values of PUF and PPF are between +0.15 and –0.6. The obtained results show that the net charge of PPPC is greater than that of PUF and PPF, indicating the high polarity of PPPC compared with PUF and PPF due to chloride atoms in its structure. The removal of Pb(II) ions from aqueous using PPPC has been examined at different pH by batch technique. The maximum removal percentages (92–100%) of Pb(II) ions occurred at pH range 3–7. This result shows that the removal process mainly depends on the electrostatic attractive forces between the metal ions (Pb^{2+}) and PPPC (–ve) at pH 5–7. While the removal of Pb(II) at pH 3–5 depends on the chelation process with reactive functional groups of PPPC.

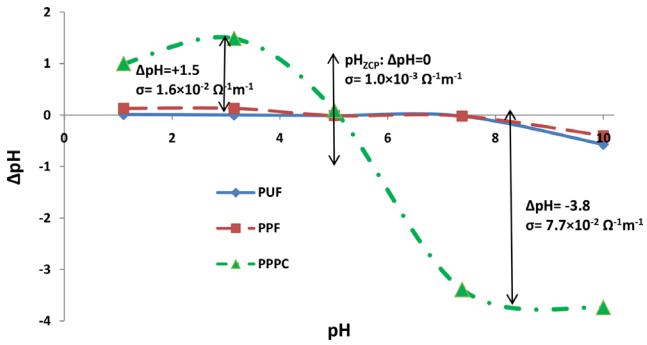

Fig. 4. pH_{PZC} of PUF, PPF and PPPC.

The electrical conductivity (σ) of PUF, PPF, and PPPC are 1.6×10^{-8}, 6.5×10^{-7} and 1.0×10^{-3} $\Omega^{-1}m^{-1}$, respectively. This

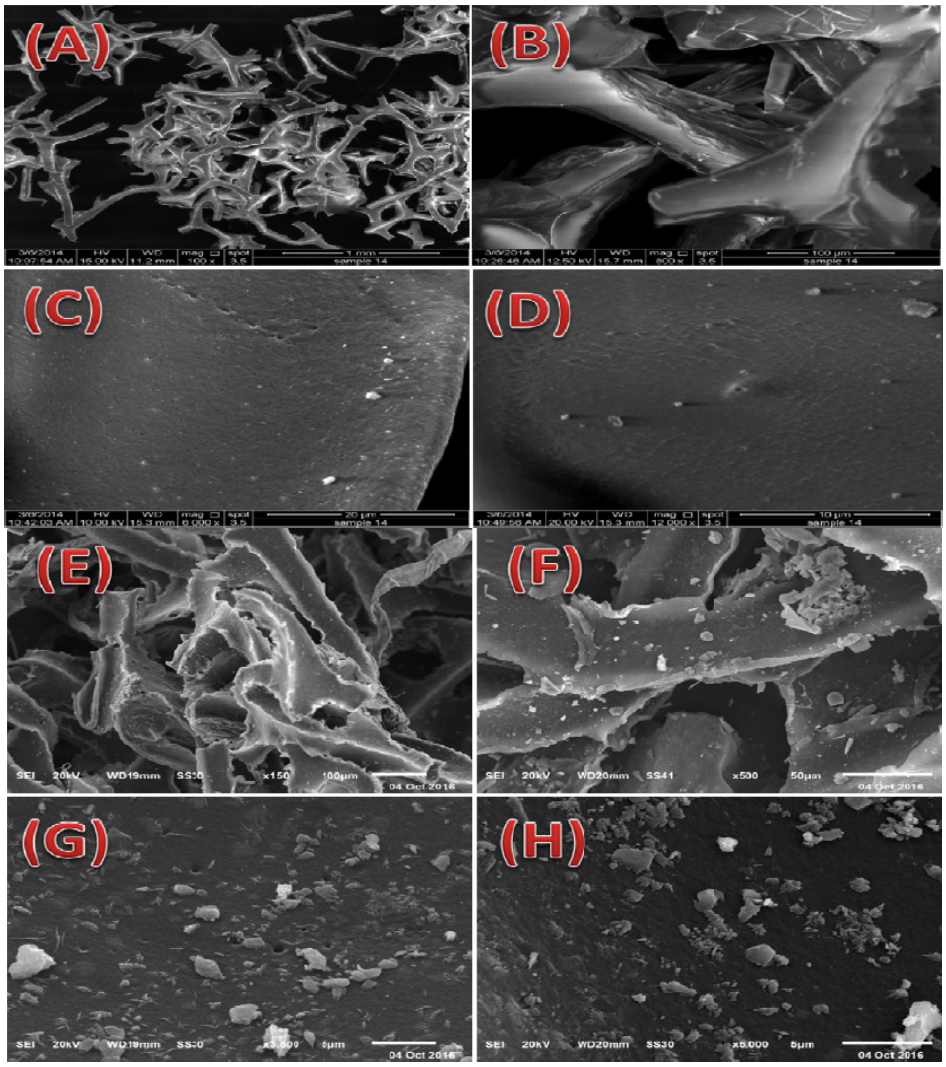

Fig. 5. Surface morphology of PPPC (A, B, C, and D) and PPPC: Pb(II) (E, F, G, and H) by SEM at magnifications of 150–12000×.

result indicates the PPPC is more polarity in the solid phase than PUF and PPF. This result discusses the ability of PPPC for attracting the metal ions according to the polarity of PPPC. The σ value was increased in an acidic and alkaline medium to 0.016 and 0.077 $\Omega^{-1}m^{-1}$; this shows that the polarity of PPPC surface was increased with pH.

The cation exchange capacity of PPPC was evaluated using methylene blue index (MBI) process [24]. The estimated cation exchange capacity of PPPC is 0.91 mmol/g (292 mg/g). PPPC exhibits better cation capacity than other sorbents e.g. Picacarb, Filtrasorb, activated carbon, coal, commercial activated carbon, bituminous coal, charcoal, activated carbon prepared from durian shell, coconut shell activated carbon, oil palm fiber-based activated carbon, olive-seed waste residue-based activated carbon, activated carbon prepared from oil palm shell [25].

Fig. 5 shows that the surface morphology of PPPC at magnifications 100×, 800×, 6000×, and 12000×. The images 5a and 5b reveal that the surface of PPPC has many spaces which are irregular in shapes, size and distribution. While the images 5c and 5d show that the PPPC surface is relatively smooth which contain many pores. These spaces and pores of PPPC would make the developed sorbent. The sorption of Pb(II) ions on the surface of PPPC was assessed by the SEM at different magnifications (150, 500, 2500 and 5000, Figs. 5E–5H). Detailed analysis of the PPPC material surface shows a deposited layer of Pb(II) ions on the surface of the PPPC and also deposited inside the spaces and holes of PPPC.

The elemental analysis (EA) of PUF, PPF, and PPPC revealed that the C, H, N, and O percentage are in the following: PUF (C: 64.7, H: 7.8, N: 7.9, O: 18.6), PPF (C: 64.3, H: 7.7, N: 7.7, O: 19.2 and PPPC (C: 62.4, H: 9.5, N: 7.5, O+Cl: 20.4). The result obtained shows that the carbon and nitrogen percentages of PPPC are lower than those of the PUF and PPF. While the hydrogen and oxygen percentages are higher than that of the PUF and PPF. These results would be due to the partial hydrolysis of urethane groups of PUF and introducing of amino, chloro, and hydroxyl groups onto the matrix and surface of PUF.

Thermal properties of PUF, PPF and PPPC were evaluated using thermogravimetric analysis (TGA), differential thermal analysis (DTA) and differential scanning calorimetry (DSC). The TGA measurements were made under a nitrogen atmosphere at a heating rate of 10°C/min from 29 to1000°C. The thermal decomposition of PUF took place at 207.1–400°C with a weight loss of 34.1 and 55.7 at the temperature ranges of 207–302 and 302–400°C, respectively [23]. While the TGA curve of PPF showed that the thermal degradation occurs through four steps at a temperature of 35–236, 237–285, 286–343 and 344–396°C with a weight loss of 0.03, 25 9, 11.9 and 61.7 [23]. On the other hand, the TGA curve of PPPC showed a smooth stepwise manner containing three steps of thermal degradation (Fig. 6A). The thermal decomposition of PPPC begins from 216°C to 474°C through five steps at the temperature ranges of 216–241, 242–292 and 293–474°C with a weight loss of 12.8, 29.0 and 58.2%. It may be suggested that the PUF and PPF matrix are fully decomposed at 400°C while the PPPC complete decomposition temperature at 474°C indicates the presence of the $–NH_2$, –OH and –Cl groups increased the thermal stability of the composite.

The DSC and DTA curves for PUF and PPF showed two endothermic peaks at 288.5 and 356.8°C and 275 and 376°C [23]. While two endothermic peaks were observed for PPPC in the DTA and DSC curves at 275 and 383°C (Fig. 6B) with enthalpy values are 148 and 60 J/g. This result shows that the PPPC matrix is relatively similar to the PPF matrix.

3.2. Kinetic studies

The time required for complete sorption of the Pb(II) ions (4 µg/L) using was 30 min. It was noticed that the initial extraction rate of Pb(II) ions is very fast, where 60% of the total Pb(II) ions concentration was removal from the tested solutions at the first 1 min. Then the rate slowed down progressively with time and the equilibrium extraction is reached within a period of 30 min.

The diffusion rates of Pb(II) ions onto PPPC were estimated using Bangham (1), Weber-Morris (2) and Reichenberg (3) equations. Where k_i (g/mmol $min^{1/2}$) is the intra particle diffusion rate coefficient, the B_t value is a mathematical function of $F = Q_t/Q_e$. D_i is the effective diffusion coefficient, and α and k_O are constant. Q_e and Q_t (mmol/g) are the sorption capacity at equilibrium and after time t (min).

$$\log\frac{C_O}{(C_O - Q_t m)} = \frac{\log k_o m}{2.303V} + \alpha \log t \tag{3}$$

$$Q_t = k_i\sqrt{t} \tag{4}$$

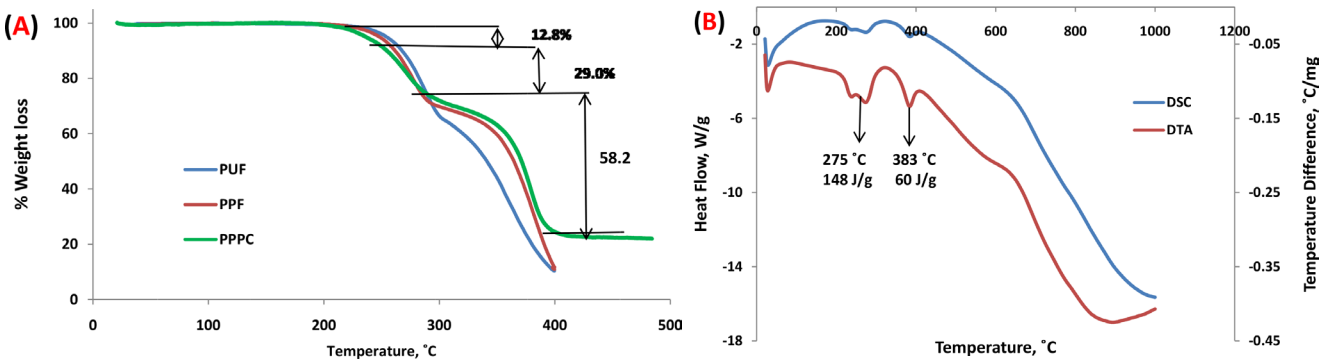

Fig. 6. (A) TGA of PUF, PPF & PPPC and (B) DTA and DSC curves of PPPC.

$$Bt = -0.4977 - \ln(1-F) \;\&\; F = \left(\frac{6}{R}\right)\left(\frac{D_i t}{\pi}\right)^{1/2} \quad (5)$$

The double logarithmic plots of Bangham equation with the time yield correlation values for removal of Pb(II) ions are 0.75, 0.94 and 0.51, respectively (Table 1). This result is showing that the diffusion of Pb(II) ions into the PPPC matrix is involved in the rate controlling step. The values α was 0.08.

The plot of $t^{1/2}$ vs. Q which gives a straight line (R^2 = 0.95), represent the intra particle diffusion model given by Morris and Weber (Eq. (2)). The particle diffusion rates (k_i) values for removing of Pb(II) ions using PPPC was 0.006 mmol g^{-1} $min^{-1/2}$. When intra particle diffusion occurs, the plot will be linear and pass through the origin and then the intra particle diffusion is a controlling step. Since the intra particle plot do not pass through the origin and relatively poor relations coefficients (R^2), the intra particle diffusion is not sol determining step.

The correlation values for the relation of t vs. Bt are 0.95 for the removal of Pb(II) ions. This indicates that the good relationship between t and Bt. Values of the effective diffusion coefficient are estimated from the plots of F vs. $t^{1/2}$. The values of D_i of the metal ions sorption was 0.05 cm^2 min^{-1}. This value shows that Reichenberg equation is the best model for the description of the diffusion mechanism.

$$\log(Q_e - Q_t) = (\log Q_e) - \left(\frac{k_1 t}{2.303}\right) \quad (6)$$

$$\frac{t}{Q_t} = \left(\frac{1}{k_2 Q_e^2}\right) + \left(\frac{t}{Q_e}\right) \quad (7)$$

The pseudo first order (4) and pseudo second order (5) kinetic models were applied to estimate the sorption rate of Pb(II) ions onto PPPC (Table 2). Where k_1(min^{-1}) and k_2 (g / mmol min) are the pseudo-first and pseudo-second order rate constant. The value of R^2 for pseudo first order sorption model 0.960 is lower than the value of R^2 for pseudo second order 0.996 this suggests that the pseudo second order adsorption mechanism is predominant and confirms the chemisorption of Pb(II) ions onto PPPC [26]. The initial rate constant ($h = k_2 Q_e^2$) was 0.103 min g/μmol for sorption of Pb(II) ions onto PPPC. The k_2 value of Pb(II) was 7.7 μmol g/min and the value of the half-life ($t_{1/2} = \frac{1}{k_2 Qe}$) was 1.13 min for the removal of Pb(II) ions using PPPC, respectively.

3.3. Thermodynamic examination

The effect of temperature (25–75°C) on the extraction of Pb(II) ions onto PPPC was studied (Table 3). The maximum extraction percentages of these metal ions were observed at low temperature; the extraction was decreased with increasing of the temperature. The thermodynamic parameters (ΔH, ΔS, and ΔG) were estimated using the following equations:

$$\ln K_c = \frac{-\Delta H}{RT} + \frac{\Delta S}{R} \quad (8)$$

$$\Delta G = \Delta H - T\Delta S \quad (9)$$

where K_c is the distribution coefficient, T is the temperature (K) and R is gas constant. The value of ΔH for the sorption Pb(II) ions was –22.9 kJ/mol; the extraction process is exothermic in nature. ΔS are –65.5 J/K mol; the negative sign of ΔS for the sorption of Pb(II) ions suggests the decrease in disorder at the solid/solution interface during the sorption process. ΔG was –3.5 kJ/mol; this value shows the spontaneous nature of the removal of the Pb(II) ions using PPPC, revealed by the negative sign of ΔG.

3.4. Equilibrium observation

The amounts of Pb(II) ions onto one gram of PPPC (Q_e) were estimated at different of Pb(II) concentrations (Table 4). The linear plots C_o vs. Q_e show that the perfect curve with R^2 value 0.967 and zero intercept (0.0001). The sorption capacities of PPPC for Pb(II) was 0.69 mmol of Pb(II) per one gram of PPPC.

The equilibrium data were analyzed using Langmuir (7) and Freundlich (8) models to explain the removal mechanism of the Pb(II) ions onto the PPPC surface. Where Q_e (mmol/g) is the adsorbed amount of metal ions at equi-

Table 1
Diffusion rate for the removal of Pb(II) using PPPC

Reichenberg model		Weber-Morris model		Bangham model	
$D_i \times 10^{-9}$	R^2	k_i	R^2	α	R^2
0.05	0.95	0.006	0.95	0.08	0.94

Table 2
Kinetic parameters of pseudo first order and pseudo second order models

Pseudo first order		Pseudo second order		h
R^2	k_1	R^2	k_2	
0.960	0.675	0.996	0.0006	7.7

Table 3
Thermodynamic parameters of the sorption Pb(II) ions onto PPPC

ΔH kJ/mol	ΔS J/mol	ΔG kJ/mol
–22.9	–65.5	–3.5

Table 4
Parameters of isotherms curve for the sorption of Pb(II) ions onto PPPC

Least square equation		Correlation coefficient, R^2	Capacity
Slope	Intercept		mmol/g
0.15	1×10^{-4}	0.98	0.69

librium, C_e (mmol/L) is the equilibrium concentration of metal ions, K_L (mmol/g) and b (L/mmol) are Langmuir constant. K_F and n are Freundlich constants.

$$\frac{C_e}{Q_c}=\left(\frac{1}{K_L b}\right)+\left(\frac{C_e}{K_L}\right) \tag{10}$$

$$\log Q=\log K_F+\tfrac{1}{n}\log C_e \tag{11}$$

The Langmuir model plot (C_e vs. C_e/Q_c) is a bad linear relationship which is confirmed by the values of the correlation coefficients (Table 5, R^2 = 0.77). While the relationship of *log* C_e vs. *log Q* due to Freundlich isotherm model is a good correlation (R^2 = 0.96). The Freundlich constant (*1/n*) was 0.8 for sorbed Pb(II) ions. The values of *1/n* are <1, which may be attributed to the heterogeneous surface structure of the PPPC with a non-uniform distribution of heat sorption over the surface. The value of *n* was 1.3, indicating that the extraction of Pb(II) ions was favorable [27].

3.5. Dynamic investigation

The flow rate of Pb(II) solutions through the PPPC column was examined to get the appropriate time of analysis. The maximum extraction percentages (100%) of these metal ions onto the PPPC column were observed at 0.5–5 mL/ min. Then the extraction percentages were decreased from 100% to 95% with an increasing flow rate from 5 to 20 mL min^{-1}.

The effect of various eluting agents (0.05 mol/L of CH_3COOH, HCl, H_2SO_4, NaOH and NH_4OH) on the recovery of Pb(II) ions from PPPC column was tested. The results show that the Pb(II) ions were completely stripping (99.2%) with 6 mL of 0.5 M CH_3COOH.

3.6. Accuracy and precision

The accuracy and precision for the extraction and recovery of the Pb(II) ions using PPPC were estimated (Table 6). The recovery percentage of Pb(II) ions is 98.8%. Also, the relative standard deviation (RSD%) for analysis seven samples replicates of these metal ions is 2.82%, indicate a good precision and accuracy of the proposed method. The estimated detection limits (LOD, n = 7) for determination of Pb(II) ions was 2.9 µg/L, this gives good precision.

Table 5
Comparison between Freundlich and Langmuir isotherm parameters

Freundlich		Langmuir	
1/*n*	R^2	K_L	R^2
0.8	0.96	0.005	0.77

Table 6
Accuracy and precision for the extraction and recovery of Pb(II) ions

Recovery	LOD	LOQ	RSD
%	µg/L	µg/L	%
98.8	2.9	9.7	2.82

3.7. Application

The validity and accuracy for the detected, estimated and removal of Pb(II) ions from water samples were successfully assessed by PPPC sorbent.

The proposed column method was applied for the addition/recovery of 25 µg of lead ions of the Pb(II) ions in Nile river water (Mansoura City), tap water (Met Khameis Plant), water well (Aga City) and wastewater (Omer Bak) samples. A 100 mL aliquot of water samples were spiked with 25 µg of the metal ions and adjusted to the optimum pH (pH 5–7). The samples were allowed to pass through the PPPC column at a flow rate of 2 mL/min and then desorbed by 0.5 mol/L CH_3COOH solution. Effluents and eluted Pb(II) ions from the PPPC column were determined by FASS. The results are given in Table 7. The removal percentages of Pb(II) from the water samples using PPPC were 99–105%. The relative standard deviation (RSD) value was 2.49% (Table 7). It shows that the PPPC column could be applied for the determination of lead ions from the different water samples.

Removal of Pb(II) from different volumes of tap water was investigated. Solutions of 10 µg of Pb(II) ions in 25–100 mL of water samples were shacked 30 min with 0.1 g of PPPC. The recovery of the Pb(II) from the PPPC was carried out by 10 mL of 0.5 M CH_3COOH then the eluates were determined. The results show that the removal percentages are 98–100% with preconcentration factors 250–1000 (RSD= 2.54%, n = 4).

4. Conclusion

The present work is concerned with the preparation of new sorbent (PPPC) containing hydroxyl group and chlorine atoms. The PPPC was used for removal of Pb(II) ions from the wastewater. The removal process is depends on polarity of PPPC. The maximum removal percentages of Pb(II) ions occurred at pH ranges 3–7. The kinetic data showed that the removal rates of these metal ions using PPPC sorbent are very rapid. The negative values of ΔG and ΔH indicated that the removal process is spontaneous and exothermic nature. This study could conclude that PPPC has the ability to extract and recovery Pb(II) ions from different real water samples.

Table 7
Determination of lead(II) ions in water samples using dynamic method

Water samples	Add	Recovery		RSD
	µg	µg	%	%
Nile river	25	24.7	98.8	2.49
Tap water	25	25	100	
Water well	25	25.8	103.2	
Wastewater	25	26.3	105.2	

References

[1] M.F. El-Shahat, E.A. Moawed, M.A.A Zaid, Preconcentration and separation of iron, zinc, cadmium and mercury, from waste water using Nile blue a grafted polyurethane foam, Talanta, 59 (2003) 851–866.

[2] W.W. Tang, G.M. Zeng, J.L. Gong, J. Liang, P. Xu, C. Zhang, B.B. Huang, Impact of humic/fulvic acid on the removal of heavy metals from aqueous solutions using nanomaterials: a review, Sci. Total Environ., 468 (2014) 1014–1027.

[3] E. Ghasemi, A. Heydari, M. Sillanpää, Super paramagnetic Fe_3O_4@ EDTA nanoparticles as an efficient adsorbent for simultaneous removal of Ag (I), Hg (II), Mn (II), Zn (II), Pb (II) and Cd (II) from water and soil environmental samples, Microchem. J., 131 (2017) 51–56.

[4] P. Bhunia, S. Chatterjee, P. Rudra, S. De, Chelating polyacrylonitrile beads for removal of lead and cadmium from wastewater, Sep. Purif. Technol., 193 (2018) 202–213.

[5] A.N. Babu, D.S. Reddy, G.S. Kumar, K. Ravindhranath, G.K. Mohan, Removal of lead and fluoride from contaminated water using exhausted coffee grounds based bio-sorbent, J. Environ. Manage., 218 (2018) 602–612.

[6] S. Ravulapalli, R. Kunta, Removal of lead (II) from wastewater using active carbon of Caryota urens seeds and its embedded calcium alginate beads as adsorbents, J. Environ. Chem. Eng., 6 (2018) 4298–4309.

[7] D.J. Leao, M.M. Junior, G.C. Brandao, S.L. Ferreira, Simultaneous determination of cadmium, iron and tin in canned foods using high-resolution continuum source graphite furnace atomic absorption spectrometry, Talanta, 153 (2016) 45–50.

[8] T. Nguyen, H. Ngo, W. Guo, J. Zhang, S. Liang, Q. Yue, Q. Li, T. Nguyen, Applicability of agricultural waste and by-products for adsorptive removal of heavy metals from wastewater, Bioresour. Technol., 148 (2013) 574–585.

[9] M.R. Pourjavid, M. Arabieh, S.R. Yousefi, A.A. Sehat, Interference free and fast determination of manganese (II), iron (III) and copper (II) ions in different real samples by flame atomic absorption spectroscopy after column graphene oxide-based solid phase extraction, Microchem. J., 129 (2016) 259–267.

[10] A. Shahbazi, H. Younesi, A. Badiei, Functionalized SBA-15 mesoporous silica by melamine-based dendrimer amines for adsorptive characteristics of Pb (II), Cu (II) and Cd (II) heavy metal ions in batch and fixed bed column, Chem. Eng. J., 168 (2011) 505–518.

[11] A.Z.M. Badruddoza, Z.B.Z. Shawon, W.J.D. Tay, K. Hidajat, M.S. Uddin, Fe_3O_4/cyclodextrin polymer nanocomposites for selective heavy metals removal from industrial wastewater, Carbohyd. Polym., 91 (2013) 322–332.

[12] M. Liu, L. Yang, L. Zhang, Functionalization of magnetic hollow porous oval shape $NiFe_2O_4$ as a highly selective sorbent for the simultaneous determination of five heavy metals in real samples, Talanta, 161 (2016) 288–296.

[13] E. Moawed, I. Ishaq, A. Abdul-Rahman, M. El-Shahat, Synthesis, characterization of carbon polyurethane powder and its application for separation and spectrophotometric determination of platinum in pharmaceutical and ore samples, Talanta, 121 (2014) 113–121.

[14] E. Moawed, M. El-Hagrasy, M. Kamal, M. El-Shahat, Recovery and determination of palladium from its alloys using iminodiacetic polyurethane/carbon nanofibers sorbent, J. Liq. Chromatogr. R. T., 39 (2016) 415–421.

[15] W. Yang, Q. Dong, S. Liu, H. Xie, L. Liu, J. Li, Recycling and disposal methods for polyurethane foam wastes, Procedia Environ. Sci., 16 (2012) 167–175.

[16] E.A. Moawed, M.A. El-Hagrasy, A.A.M. Farhat, Application of the magnetic isothiouronium polyurethane sorbent for removal of acidic and basic dyes from wastewater, J. Clean. Prod., 157 (2017) 232–242.

[17] E. Moawed, A. Abulkibash, M. El-Shahat, Synthesis of tannic acid azo polyurethane sorbent and its application for extraction and determination of atrazine and prometryn pesticides in foods and water samples, Environ. Nanotechnol. Monit. Manag., 3 (2015) 61–66.

[18] J.O. Vinhal, A.D. Gonçalves, G.F. Cruz, R.J. Cassella, Speciation of inorganic antimony (III & V) employing polyurethane foam loaded with bromopyrogallol red, Talanta, 150 (2016) 539–545.

[19] E.A. Moawed, H.A. Kiwaan, M.M. Elshazly, Application of polyurethane@salvadora persica composite for detection and removal of acidic and basic dyes from wastewater, J. Taiwan Inst. Chem. Eng., 80 (2017) 894–900.

[20] E. Moawed, A. Radwan, Application of acid modified polyurethane foam surface for detection and removing of organochlorine pesticides from wastewater, J. Chromatogr. B., 1044 (2017) 95–102.

[21] E. Moawed, A. Abulkibash, M. El-Shahat, Synthesis and characterization of iodo polyurethane foam and its application in removing of aniline blue and crystal violet from laundry wastewater, J. Taibah Univ. Sci., 9 (2015) 80–88.

[22] E. Moawed, M. El-Hagrasy, N. Embaby, Substitution influence of halo polyurethane foam on the removal of bismuth, cobalt, iron and molybdenum ions from environmental samples, J. Taiwan Inst. Chem. Eng., 70 (2017) 382–390.

[23] E. Moawed, M. El-Shahat, Synthesis, characterization of low density polyhydroxy polyurethane foam and its application for separation and determination of gold in water and ores samples, Anal. Chim. Acta, 788 (2013) 200–207.

[24] H. Tounsadi, A. Khalidi, M. Abdennouri, N. Barka, Activated carbon from Diplotaxis Harra biomass: optimization of preparation conditions and heavy metal removal, J. Taiwan Inst. Chem. Eng., 59 (2016) 348–358.

[25] M. Rafatullah, O. Sulaiman, R. Hashim, A. Ahmad, Adsorption of methylene blue on low-cost adsorbents: a review, J. Hazard. Mater., 177 (2010) 70–80.

[26] M.H. Kalavathy, T. Karthikeyan, S. Rajgopal, L.R. Miranda, Kinetic and isotherm studies of Cu (II) adsorption onto H_3PO_4-activated rubber wood sawdust, J. Colloid Interface Sci., 292 (2005) 354–362.

[27] A.S. Özcan, A. Özcan, Adsorption of acid dyes from aqueous solutions onto acid-activated bentonite, J. Colloid Interface Sci., 276 (2004) 39–46.